

# **Niobium Dioxide Prepared by a Novel La-reduced Route as Promising Catalyst Support for Pd towards Oxygen Reduction Reaction**

Chong Huang,<sup>ab</sup> Wujie Dong,<sup>\*a</sup> Chenlong Dong,<sup>c</sup> Xin Wang,<sup>d</sup> Bingquan Jia<sup>ab</sup> and Fuqiang Huang<sup>\*abc</sup>

<sup>a</sup> State Key Laboratory of High Performance Ceramics and Superfine Microstructure, Shanghai Institute of Ceramics, Chinese Academy of Sciences, Shanghai 200050, P. R. China

<sup>b</sup> University of Chinese Academy of Sciences, Beijing 100049, China

<sup>c</sup> State Key Laboratory of Rare Earth Materials Chemistry and Applications, College of Chemistry and Molecular Engineering, Peking University, Beijing 100871, P.R. China

<sup>d</sup> College of Chemistry and Molecular Engineering, Zhengzhou University, Zhengzhou, 450001, China

## **Experimental section**

### **Synthesis of Nb<sub>2</sub>O<sub>5</sub> nanoparticles**

All reagents were highly pure and used without further purification. Nb<sub>2</sub>O<sub>5</sub> nanoparticles were prepared by hydrothermal method. Initially, 4 g ammonium niobite oxalate hydrate and 12 g urea were dissolved in 155 mL pure water with 5 mL acetic acid and then stirred for 2 h. Secondly, the mixed solution was transferred into a 200 mL Teflon-lined autoclave, which was subsequently sealed and placed in an oven at 160 °C for 12 h. The white precipitate was collected by washing and filtering, and then

dried at 60 °C in air. Finally, the precipitate was annealed at 500 °C for 4 h and Nb<sub>2</sub>O<sub>5</sub> nanoparticles were obtained.

### **Synthesis of NbO<sub>2</sub> nanoparticles**

As-prepared Nb<sub>2</sub>O<sub>5</sub> nanoparticles were mixed with lanthanum powders prior to being sealed in a quartz tube and calcined at 500 °C for 6 h. The specific procedure was as follows: 0.25 g Nb<sub>2</sub>O<sub>5</sub> nanoparticles and 1 g La powders were mixed and homogenized by grinding. Next, the powder mixture was transferred into a quartz tube which was subsequently sealed and kept in an oven at 500 °C for 6 h. After cooling, the product was immersed in diluted hydrochloric acid solution to remove La<sub>2</sub>O<sub>3</sub> and unreacted La. Lastly, the sediments were obtained by filtration and washed with de-ionized water for several times. After dried in an oven at 60 °C for 6 h, the NbO<sub>2</sub> nanoparticles were synthesized eventually.

### **Synthesis of Pd/NbO<sub>x</sub> composite**

In a typical synthesis, 50 mg as-obtained NbO<sub>x</sub> nanoparticles and 5 mg PVP were distributed in 40 mL deionized water. Then, 2.10 mL 0.0564 M PdCl<sub>2</sub> aqueous solution was added into the above solution. After stirring overnight, 10 mL 0.05 M NaBH<sub>4</sub> was added into the solution in order to reduce the Pd<sup>2+</sup> into Pd. Subsequently, the solution was filtered and the black precipitate was washed several times with deionized water and ethanol so as to remove the residual NaBH<sub>4</sub> and byproducts (e.g. NaCl, H<sub>3</sub>BO<sub>3</sub>). Ultimately, the Pd/NbO<sub>x</sub> composite was obtained after the precipitate was dried at 60 °C in air.

## Material Characterization

Powder X-ray diffraction data of all these samples were collected by using a Bruker D8 Advance diffractometer equipped with Cu K $\alpha$  radiation ( $\lambda = 1.5405 \text{ \AA}$ ). Morphologies of samples were observed on a JEOL-2100F Transmission electron microscopy (TEM) operated at an acceleration voltage of 200 kV. Raman spectra were collected on a LabRAM HR Evolution spectrometer using a laser with an excitation wavelength of 532 nm at laser power of 10 mW. X-ray photoelectron spectroscopy (XPS) experiments was carried out on the RBD upgraded PHI-5000C ESCA system (PerkinElmer) with Mg K  $\alpha$  radiation ( $h\nu = 1253.6 \text{ eV}$ ). Resistivity of the as-prepared NbO<sub>2</sub> at room temperature was measured on a Physical Properties Measurement System (PPMS, Quantum Design). Resistivity of the pristine Nb<sub>2</sub>O<sub>5</sub> was estimated by current-voltage (I-V) measurements which was performed by sweeping the voltage from the positive maximum to the negative minimum using a semiconductor characterization system (Keithley 4200).

## Electrochemical measurements

ORR catalytic activity of samples was carried out with a conventional three-electrode configuration using rotating disk electrode (RDE) coating with a film of catalyst as the working electrode, saturated calomel electrode (SCE) as the reference electrode and carbon electrode as the counter electrode, 0.1 M KOH solution as the electrolyte. As for the preparation of the working electrode, 5 mg of catalyst and 1 mg of acetylene black were dispersed in 1 mL of Nafion/alcohol solution (0.5 wt. %) by sonication for 60 min to form 5.0 mg mL<sup>-1</sup> slurry. Then, 10  $\mu$ L of slurry was pipetted onto the polished

RDE in order to obtain a film of catalyst (loading mass of 250  $\mu\text{g cm}^{-2}$ ). All the data were recorded by a CHI660E Electrochemical Workstation (Chenhua, Shanghai).

Oxygen reduction performances of the samples were detected in 0.1 M KOH solution de-aerated by oxygen through cyclic voltammetry at scan rate of 100  $\text{mV s}^{-1}$  and linear sweep voltammetry at scan rate of 10  $\text{mV s}^{-1}$  under various rotating speeds. The reference electrode was calibrated for the reversible hydrogen potential. The current density was the ratio of current to geometric surface area of rotating disk electrode ( $0.19635 \text{ cm}^2$ ). The presented LSV curves were corrected for the ohmic potential drop losses. Onset potential was determined to be the potential value corresponding to 5% of the diffusion-limited current in this work.<sup>1, 2</sup> Kouteckey-Levich plots showing the linear relation between  $J^{-1}$  and  $\omega^{-1/2}$  were obtained based on the following equations:

$$\frac{1}{J} = \frac{1}{J_k} + \frac{1}{B\omega^{1/2}}$$

$$B = 0.62nFC_0(D_0)^{2/3}\nu^{1/6}$$

where  $J$  is the current density,  $J_k$  is the kinetic current density,  $\omega$  is the rotating rate of the working electrode,  $F$  is the Faraday constant ( $96485 \text{ C mol}^{-1}$ ),  $n$  is the electron transfer number,  $C_0$  is the solubility of oxygen in the electrolyte ( $1.2 \times 10^{-3} \text{ mol L}^{-1}$ ),  $D_0$  is the diffusion coefficient ( $\text{O}_2$ ,  $1.9 \times 10^{-5} \text{ cm}^2 \text{ s}^{-1}$ ), and  $\nu$  is the kinematic viscosity of the electrolyte ( $0.01 \text{ cm}^2 \text{ s}^{-1}$ ) for the case of 0.1 M KOH solution.<sup>3</sup>

In addition, the electron transfer numbers ( $n$ ) and the peroxide yields ( $\text{H}_2\text{O}_2$  %) of Pd/NbO<sub>2</sub> were further precisely determined by the rotating ring-disk electrode (RRDE) measurements. And the detailed values for  $n$  and  $\text{H}_2\text{O}_2$  % were calculated from the following equations:

$$n=4\times\frac{I_d}{I_d+\frac{I_r}{N}}$$

$$\text{H}_2\text{O}_2(\%)=200\times\frac{\frac{I_r}{N}}{I_d+\frac{I_r}{N}}$$

where  $I_r$  and  $I_d$  are the ring and disk current, respectively.  $N$  (0.37) is the current collection efficiency of the Pt ring in RRDE.<sup>4</sup>

To investigate the long-term stability of Pd/NbO<sub>2</sub>, the test was carried out by taking continuous potential cycling in the potential window of 0.21 V to ~ 1.21 V (*vs.* RHE) at a scan rate of 100 mV s<sup>-1</sup>. After potential cycling, the LSV curve was recorded at a scan rate of 10 mV s<sup>-1</sup>. Moreover, the chronoamperometric test (current *versus* time) for Pd/NbO<sub>2</sub> and Pd/C was executed under 0.37 V (*vs.* RHE).

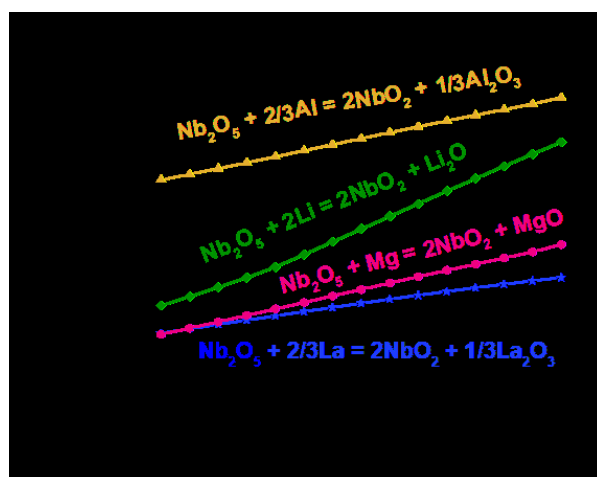


**Figure S1.**  $\Delta G^0$ -Ellingham diagram of reduction reaction for different metals and  $\text{Nb}_2\text{O}_5$  (data from the HSC chemistry).

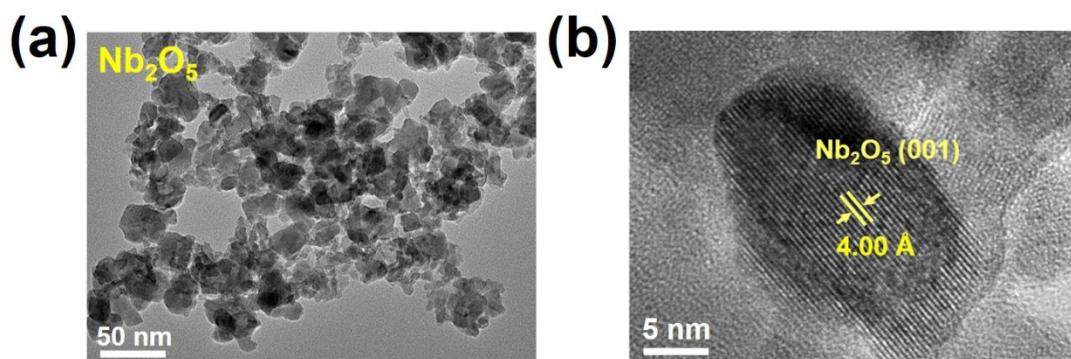


**Figure S2.** (a) TEM image and (b) HRTEM image of pristine  $\text{Nb}_2\text{O}_5$ .

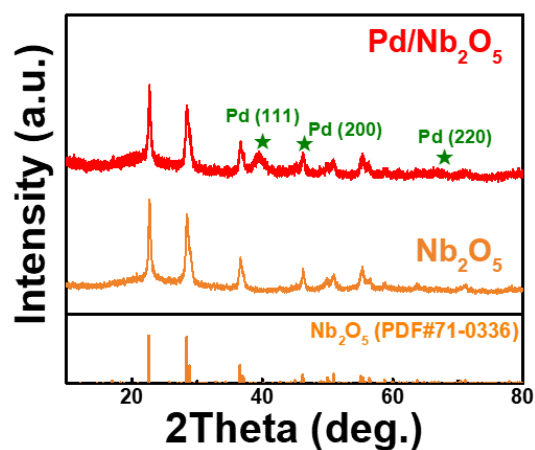


**Figure S3.** XRD patterns of  $\text{Pd}/\text{Nb}_2\text{O}_5$  composite.

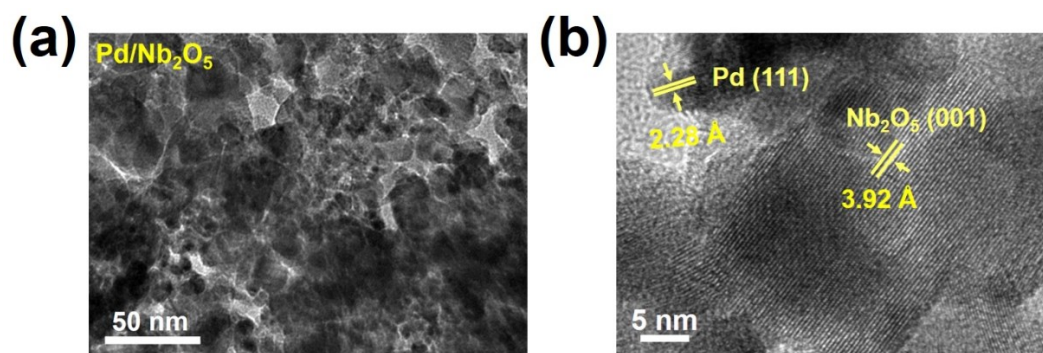


**Figure S4.** (a) TEM image and (b) HRTEM image of Pd/Nb<sub>2</sub>O<sub>5</sub>.

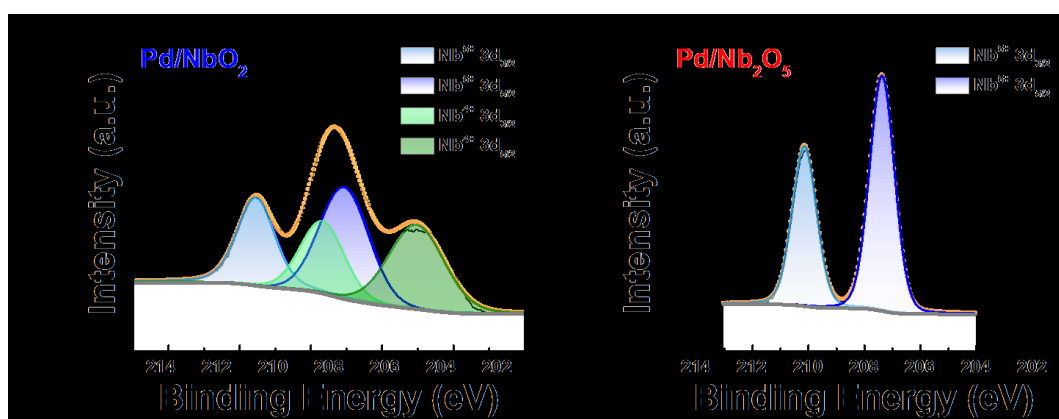


**Figure S5.** X-ray photoelectron spectrum of Nb 3d region in (a) Pd/NbO<sub>2</sub> and (b) Pd/Nb<sub>2</sub>O<sub>5</sub>.

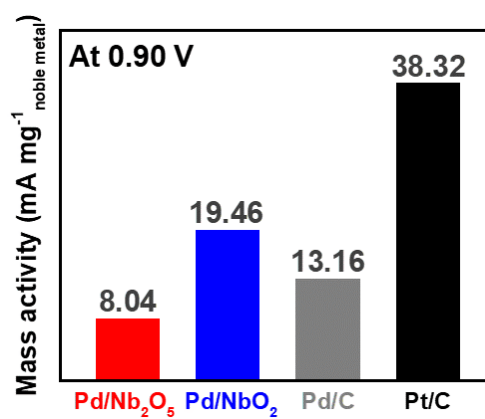


**Figure S6.** Corresponding mass activities of all the catalysts at 0.90 V (vs. RHE).

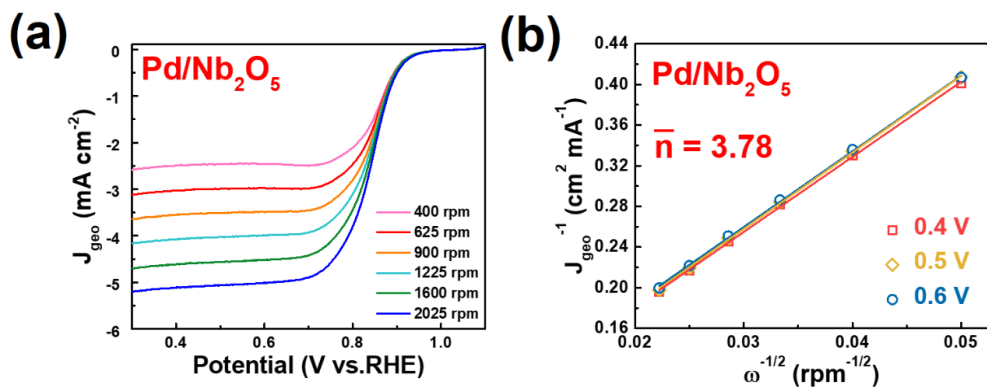


**Figure S7.** (a) LSV curves of Pd/NbO<sub>2</sub> at different rotation speeds; (b) K-L plots for Pd/NbO<sub>2</sub> derived from (a).

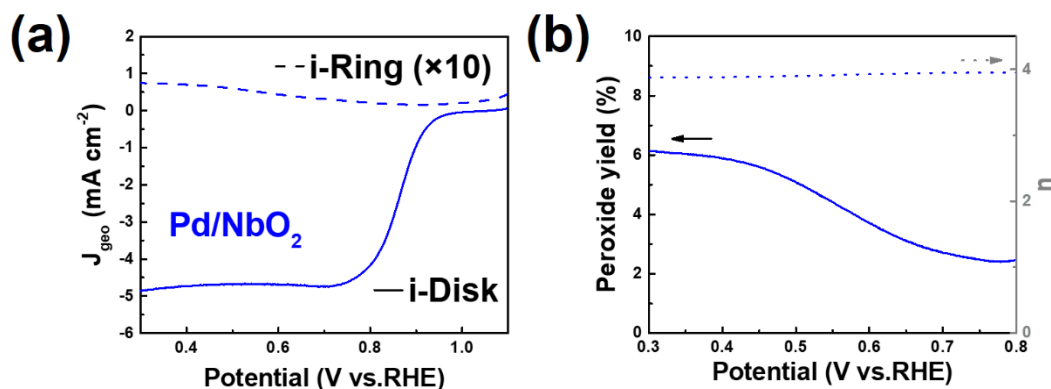


**Figure S8.** (a) RRDE voltammograms of Pd/NbO<sub>2</sub>; (b) Peroxide yield of Pd/NbO<sub>2</sub> during the ORR process (solid line) and the calculated electron transfer number (dot line) derived from (a).

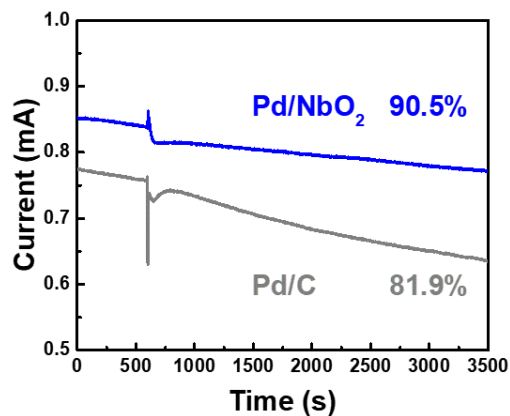


**Figure S9.** Chronoamperometric curves of Pd/NbO<sub>2</sub> and Pd/C catalysts at 0.37 V (vs. RHE) with addition of CH<sub>3</sub>OH after 600 s.



**Table S1.** Electrical conductivity of NbO<sub>2</sub> and Nb<sub>2</sub>O<sub>5</sub> at room temperature.

Sample	Electric conductivity (S/m)
NbO <sub>2</sub>	$2.95 \times 10^{-3}$
Nb <sub>2</sub> O <sub>5</sub>	$8.89 \times 10^{-7}$

**Table S2.** Comparison of ORR catalytic activity between Pd/NbO<sub>2</sub> and Pd-based catalysts in the alkaline electrolytes.

Catalyst	Half-wave potential (V vs.RHE)	Reference
Pd/NbO <sub>2</sub>	0.872	This work
Pd/TiO <sub>2-x</sub> N	0.81	3
Ni@Pd <sub>3</sub> /C	0.86	5
Au <sub>10</sub> Pd <sub>40</sub> Co <sub>50</sub>	0.83	6
PdFS-CSNS	0.892	7
Ni@Pd-rGO	0.8138	8
Pd-Ru@NG	0.8	9
Pd <sub>3</sub> Pb SNP	0.887	10
Ordered PaCuCo NPs/C	0.872	11
Ordered PaCuNi NPs/C	0.862	11
Pd/W <sub>18</sub> O <sub>49</sub>	0.875	12
Icosahedral Pd <sub>6</sub> Ni/C	0.89	13

**Table S3.** Noble metal content in Pd/NbO<sub>2</sub>, Pd/Nb<sub>2</sub>O<sub>5</sub>, commercial Pd/C and Pt/C obtained from ICP-OES.

Sample	Noble metal content (wt %)
Pd/NbO <sub>2</sub>	21.39
Pd/Nb <sub>2</sub> O <sub>5</sub>	21.95
Commercial Pd/C	17.08
Commercial Pt/C	17.86

## Reference:

1. W. Xia, A. Mahmood, Z. Liang, R. Zou and S. Guo, *Angew. Chem., Int. Ed.*, 2016, **55**, 2650-2676.
2. L. Birry, J. H. Zagal and J.-P. Dodelet, *Electrochem. Commun.*, 2010, **12**, 628-631.
3. X. T. Yuan, X. Wang, X. Y. Liu, H. X. Ge, G. H. Yin, C. L. Dong and F. Q. Huang, *ACS Appl. Mater. Interfaces*, 2016, **8**, 27654-27660.
4. L. Lv, D. Zha, Y. Ruan, Z. Li, X. Ao, J. Zheng, J. Jiang, H. M. Chen, W.-H. Chiang and J. Chen, *ACS Nano*, 2018, **12**, 3042-3051.
5. J. Jiang, H. Gao, S. Lu, X. Zhang, C.-Y. Wang, W.-K. Wang and H.-Q. Yu, *J. Mater. Chem. A*, 2017, **5**, 9233-9240.
6. K. A. Kuttiyiel, K. Sasaki, D. Su, L. Wu, Y. Zhu and R. R. Adzic, *Nat. Commun.*, **5**, 5185.
7. M. Yusuf, M. Nallal, K. M. Nam, S. Song, S. Park and K. H. Park, *Electrochim. Acta*, 2019, **325**, 134938.
8. F. Wang, J. Qiao, J. Wang, H. Wu, Z. Wang, W. Sun and K. Sun, *J. Alloys Compd.*, 2019, **811**, 151882.
9. B. K. Barman, B. Sarkar and K. K. Nanda, *Chem. Commun.*, 2019, **55**, 13928-13931.
10. K. Wang, Y. Qin, F. Lv, M. Li, Q. Liu, F. Lin, J. Feng, C. Yang, P. Gao and S. Guo, *Small Methods*, 2018, **2**, 1700331.
11. K. Jiang, P. Wang, S. Guo, X. Zhang, X. Shen, G. Lu, D. Su and X. Huang, *Angew. Chem., Int. Ed.*, 2016, **55**, 9030-9035.
12. Y. Lu, Y. Jiang, X. Gao, X. Wang and W. Chen, *J. Am. Chem. Soc.*, 2014, **136**, 11687-11697.
13. Y. Feng, Q. Shao, Y. Ji, X. Cui, Y. Li, X. Zhu and X. Huang, *Sci. Adv.*, 2018, **4**, eaap8817.